

- CHIHARA, H., NAKAMURA, N. & TACHIKI, M. (1973). *J. Chem. Phys.* **59**, 5387-5391.
- CHU, S. S. C., JEFFREY, G. A. & SAKURAI, T. (1962). *Acta Cryst.* **15**, 661-671.
- DUNN, A. G., RAHMAN, A. & STAVELEY, L. A. K. (1978). *J. Chem. Thermodyn.* **10**, 787-796.
- EHRENFEST, P. (1933). *Proc. Acad. Sci. Amsterdam*, **36**, 153-157.
- ELLENSON, W. D. & KJEMS, J. K. (1977). *J. Chem. Phys.* **67**, 3619-3623.
- HERBSTEIN, F. H. (1971). In *Perspectives in Structural Chemistry*, edited by J. D. DUNITZ & J. A. IBERS, Vol. IV, pp.166-395. London and New York: John Wiley.
- HERBSTEIN, F. H., MARSH, R. E. & SAMSON, S. (1994). *Acta Cryst.* **B50**, 174-181.
- HERBSTEIN, F. H. & SNYMAN, J. A. (1969). *Philos. Trans. R. Soc. London Ser. A*, **264**, 635-666.
- JESSEN, S. M. & KÜPPERS, H. (1990). *Z. Krist. Collected Abstracts of XIIth European Crystallographic Meeting, Moscow*, Vol. I, p. 349 (published as Supplement No. 2 of 1990).
- JESSEN, S. M. & KÜPPERS, H. (1991). *J. Appl. Cryst.* **24**, 239-241.
- LEFEBVRE, J., ODOU, G., MÜLLER, M., MIERZEJEWski, A. & LUTY, T. (1989). *Acta Cryst.* **B45**, 323-336.
- LIFSHITZ, E. M. & PITAEVSKII, L. P. (1980). In *Course of Theoretical Physics*, 3rd ed., *Statistical Physics*, Part 1, Vol. 5, ch. 10, edited by L. D. LANDAU, & E. M. LIFSHITZ. Oxford: Pergamon Press.
- NYE, J. F. (1967). *Physical Properties of Crystals*, 1st ed. Oxford: Clarendon Press.
- PARSONAGE, N. G. & STAVELEY, L. A. K. (1978). *Disorder of Crystals*. New York: Oxford Univ. Press.
- PIPPARD, A. B. (1964). *The Elements of Classical Thermodynamics*. Cambridge: Cambridge Univ. Press.
- RICHARDSON, C. B. (1963). *J. Chem. Phys.* **38**, 510-515.
- SALJE, E. K. H. (1990). *Phase Transitions in Ferroelastic and Co-elastic Crystals, Cambridge Topics in Mineral Physics and Chemistry*. Cambridge: Cambridge Univ. Press.
- SAMSON, S., GOLDISH, E. & DICK, C. J. (1980). *J. Appl. Cryst.* **13**, 425-432.
- SEKI, M., MATSUO, T. & SUGA, H. (1990). *J. Incl. Phenom. Mol. Recogn. Chem.* **9**, 243-251.
- STANLEY, H. E. (1971). *Introduction to Phase Transitions and Critical Phenomena*. Oxford: Oxford Univ. Press.
- STOKES, H. T. & HATCH, D. M. (1988). *Isotropy Subgroups of the 230 Crystallographic Space Groups*. Singapore: World Scientific.
- SUZUKI, K. & SEKI, S. (1953). *Bull. Chem. Soc. Jpn.* **26**, 372-380.
- SVENSSON, C. & ABRAHAMS, S. C. (1986). *Acta Cryst.* **B42**, 280-286.
- TAYLOR, R. & KENNARD, O. (1986). *Acta Cryst.* **B42**, 112-120.
- TERAUCHI, H., SAKAI, T. & CHIHARA, H. (1975). *J. Chem. Phys.* **62**, 3832-3833.
- TOLEDANO, J.-C. & TOLEDANO, P. (1987). *The Landau Theory of Phase Transitions*. Singapore: World Scientific.
- WEPEREN, K. J. VAN & VISSER, G. J. (1972). *Acta Cryst.* **B28**, 338-342.
- WONG, W.-K. & WESTRUM, E. F. JR (1971). *J. Chem. Thermodyn.* **3**, 105-124.

Acta Cryst. (1994). **B50**, 191-200

Pyridinium Picrate – the Structures of Phases I and II. Correction of Previous Report for Phase I. Study of the Phase Transformation

BY MARK BOTOSHANSKY, FRANK H. HERBSTEIN AND MOSHE KAPON

Department of Chemistry, Technion-Israel Institute of Technology, Haifa 32000, Israel

(Received 5 February 1993; accepted 11 August 1993)

Abstract

Pyridinium picrate, $C_5H_6N^+ \cdot C_6H_2N_3O_7^-$, was reported [Kofler (1944). *Z. Elektrochem.* **50**, 200-207] to exist in two crystalline phases, one (I) being stable below 343 K and the other (II) between 343 K and the melting point (~438 K). The room-temperature structure of phase I, studied by two-dimensional methods, has been reported [Talukdar & Chaudhuri (1976). *Acta Cryst.* **B32**, 803-808]. We were led to reinvestigate the system by a number of unusual features in Kofler's description of the phase behaviour. Single crystals of phase I were grown from solution and those of phase II from the melt. We have determined the structure of both phases, including analysis of the thermal motion of the picrate ions, which was found to be appreciably larger in phase II than in phase I. The reported structure of phase I was found to be incorrect, although there were no warning signs; the error was caused by confusion

between a centre and twofold screw axis in projection down [010]. The packing units in the two phases are nearly identical and consist of hydrogen-bonded cation-anion pairs. These are packed in stacks, with the ion-pairs superimposed in parallel array in phase I whereas those in phase II are antiparallel; the transition between the two phases, therefore, cannot be expected to be single crystal to single crystal, as indeed it is not. Differential scanning calorimetry (DSC) and variable-temperature powder X-ray diffraction photography show that the transition occurs at 383 K. Kofler appears to have been misled by a colour change in the phase I crystals at 343 K, which we have also observed but cannot explain. The DSC measurements give $\Delta H_{trans} = 6.8 \text{ kJ mol}^{-1}$ and $\Delta H_{fus} = 31.2 \text{ kJ mol}^{-1}$. The transition has proved not to be reversible under our experimental conditions; for example, phase II crystals remain unchanged after 24 h at 353 K. This suggests that the temperature at which the crystalline phases

are in thermodynamic equilibrium is appreciably below 383 K; we have not been able to determine the transition temperature. The details of the structure determinations (both at 298 K) are as follows: phase I, $M_r = 308.22$, $\lambda(\text{Mo } K\alpha) = 0.71069 \text{ \AA}$, $F(000) = 632$, yellow laths, monoclinic, $\mu(\text{Mo } K\alpha) = 0.95 \text{ cm}^{-1}$, $P2_1/c$, $a = 12.122 (2)$, $b = 3.783 (1)$, $c = 26.621 (3) \text{ \AA}$, $\beta = 92.56 (5)^\circ$, $V = 1219.6 \text{ \AA}^3$, $Z = 4$, $D_m = 1.62$ (floatation at 298 K), $D_x = 1.67 \text{ g cm}^{-3}$, $R_{\text{int}} = 0.0167$ (based on 25 pairs of equivalent reflections), $R_F = 0.0436$, $wR = 0.0492$ [based on 1645 independent reflections with $F > 3\sigma(F)$], refinement on F ; phase II, $M_r = 308.22$, $\lambda(\text{Mo } K\alpha) = 0.71069 \text{ \AA}$, $F(000) = 316$, yellow prisms, triclinic, $\mu(\text{Mo } K\alpha) = 0.90 \text{ cm}^{-1}$, $P\bar{1}$, $a = 10.156 (2)$, $b = 8.984 (2)$, $c = 7.230 (1) \text{ \AA}$, $\alpha = 86.38 (5)$, $\beta = 80.10 (5)$, $\gamma = 89.97 (5)^\circ$, $V = 648.6 \text{ \AA}^3$, $Z = 2$, $D_m = 1.60$ (floatation at 298 K), $D_x = 1.58 \text{ g cm}^{-3}$, $R_F = 0.0716$, $wR = 0.0694$ [based on 1478 independent reflections with $F > 3\sigma(F)$], refinement on F . Cell dimensions have been measured as a function of temperature for both phases.

1. Introduction

Pyridinium picrate was reported by Kofler (1944) to be dimorphic, with an enantiotropic transformation point at 343 K. The polymorph stable at room temperature (phase I - our nomenclature, opposite to that of Kofler) was reported to melt (on rapid heating) at 408 K, and the high-temperature form (phase II) at 438 K. Kofler also reported that if phase I is heated for a long (but unspecified) time at 393 K, then phase II is obtained on recrystallization, a result we have not been able to confirm.

The structure of phase I at room temperature has been reported from two-dimensional analysis (Talukdar & Chaudhuri, 1976; abbreviated as TC76). However, our present three-dimensional analysis shows that there are errors in this structure. We report the corrected structure and consider how this error could so far have passed undetected. We have grown single crystals of phase II and report its structure at room temperature. Pyridinium picrate appears in both phases as an internally linked hydrogen-bonded ion pair and both phases are thus molecular crystals, rather than salts, as far as their structural arrangements are concerned. We report the determinations of the two crystal structures separately, but discuss the results obtained together, thus facilitating their comparison. Some aspects of the phase transformation have also been studied.

The crystal structures of many picrates have been determined with high standards of precision and this provides a database, already used by Walkinshaw (1986), for comparison of the dimensions and conformation of the picrate ion in different crystallographic environments. We extend this comparison by including more recent structures reported for picrate ions.

2. Determination of the crystal structure of phase I

2.1. Experimental

Pyridinium picrate was prepared by reaction of equimolar amounts of pyridine and picric acid in ethanol. Long yellow laths of phase I, elongated along [010], were obtained by slow cooling from $\sim 313 \text{ K}$. These crystals melted, after transformation, at 441 K, in good agreement with literature values. After preliminary diffraction photography (Ni-filtered $\text{Cu } K\alpha$), cell dimensions and space group were determined on a Philips PW 1100 four-circle diffractometer (graphite-monochromated $\text{Mo } K\alpha$) using a crystal of dimensions approximately $0.13 \times 0.24 \times 0.4 \text{ mm}$, set with [010] approximately along φ . 25 reflections with $10 \leq 2\theta \leq 30^\circ$ were used for the cell-dimension determination; our results agree well with those of TC76. In all 2576 reflection intensities were measured by the $\omega/2\theta$ scan method; the maximum value of $\sin \theta/\lambda = 0.595 \text{ \AA}^{-1}$ and the indices lay within the limits $-14 \leq h \leq 14$, $0 \leq k \leq 4$, $0 \leq l \leq 30$. 425 reflections were rejected as deriving from space-group absences and a further 50 were removed as redundant after having been used to calculate R_{int} . Absorption corrections were not applied. Intensities of three standard reflections were measured at intervals of 120 min; crystal and measuring systems were stable to within 1% over the 48 h measuring period. The structure was solved by direct methods using *SHELXS86* (Sheldrick, 1986) and refined (on F) by *SHELX76* (Sheldrick, 1976) in its standard form, using 1645 independent reflections with $F > 3\sigma(F)$; anisotropic displacement factors were refined for non-H atoms and isotropic displacement factors for H atoms. The final weighting scheme was $w = 1/[\sigma^2(F_{\text{meas}}) + 0.00193(F_{\text{meas}})^2]$. The final R_F value was 0.0436; 231 parameters were refined. The largest value of $|\Delta/\sigma|$ in the final refinement cycle was 0.09 (average value 0.023), and ρ_{max} and ρ_{min} in the final difference map were 0.17 and -0.23 e \AA^{-3} , respectively. Atomic parameters are in Table 1.*

2.2. Comparison with results of TC76

Our x and z atomic coordinates agree reasonably well with those of TC76, except that their values are incremented by ~ 0.5 and ~ 0.25 , respectively, with respect to ours. The increment of $1/4$ in z means that TC76 chose the origin of their cell along a twofold screw axis instead of at a centre of symmetry, the two situations being indistinguishable in projection along [010] but not in three dimensions. This is a classical type

* Lists of observed and calculated structure factors, anisotropic temperature factors, deviations from best planes, intermolecular contacts below 3.4 Å and variations of cell dimensions with temperature have been deposited with the British Library Document Supply Centre as Supplementary Publication No. SUP 71556 (25 pp.). Copies may be obtained through the Executive Secretary, International Union of Crystallography, 5 Abbey Square, Chester CH1 2HU, England. [CIF reference: MU0308]

Table 1. Atomic parameters ($\times 10^4$) for phase I of pyridinium picrate [pyridinium C(1)P to H(NP); picrate C(1) to H(2)]

The values of U_{eq} (units of 10^{-4} \AA^2) were calculated following Fischer & Tillmanns (1988) and their e.s.d.'s following the isotropic and orthic approximation of Schomaker & Marsh (1983). The values of U_{iso} also have units of 10^{-4} \AA^2 .

	<i>x</i>	<i>y</i>	<i>z</i>	U_{eq}/U_{iso}
C(1)	2809 (2)	7464 (6)	1258 (1)	336 (5)
C(2)	1734 (2)	6094 (7)	1370 (1)	313 (5)
C(3)	1371 (2)	5659 (7)	1850 (1)	326 (5)
C(4)	2054 (2)	6624 (6)	2255 (1)	324 (5)
C(5)	3108 (2)	7924 (5)	2190 (1)	333 (5)
C(6)	3460 (2)	8315 (6)	1712 (1)	321 (5)
N(1)	964 (2)	5098 (6)	963 (1)	389 (5)
O(1)	1078 (2)	6272 (6)	538 (1)	633 (6)
O(2)	210 (2)	3093 (6)	1057 (1)	601 (5)
N(2)	1664 (2)	6297 (6)	2759 (1)	405 (5)
O(3)	818 (2)	4635 (6)	2823 (1)	602 (6)
O(4)	2206 (2)	7700 (7)	3102 (1)	648 (6)
N(3)	4584 (2)	9637 (6)	1665 (1)	404 (5)
O(5)	5289 (2)	8686 (7)	1981 (1)	644 (6)
O(6)	4770 (2)	11646 (5)	1319 (1)	574 (5)
O(7)	3168 (2)	7754 (6)	828 (1)	496 (5)
H(1)	736 (25)	4759 (79)	1895 (10)	480 (80)
H(2)	3554 (21)	8556 (73)	2471 (9)	380 (70)
NP	2572 (2)	10528 (6)	-49 (1)	382 (5)
C(1)P	3589 (2)	11747 (7)	-102 (1)	415 (6)
C(2)P	3884 (2)	13082 (8)	-553 (1)	452 (6)
C(3)P	3098 (2)	13148 (8)	-950 (1)	467 (6)
C(4)P	2059 (2)	11942 (8)	-879 (1)	457 (7)
C(5)P	1799 (2)	10588 (7)	-418 (1)	421 (6)
H(1)P	4065 (24)	11474 (77)	192 (10)	510 (80)
H(2)P	4613 (28)	13843 (88)	-611 (12)	630 (90)
H(3)P	3320 (26)	14216 (94)	-1278 (12)	670 (90)
H(4)P	1494 (23)	11846 (75)	-1136 (10)	480 (80)
H(5)P	1092 (27)	9603 (85)	-340 (11)	550 (80)
H(NP)	2420 (25)	9744 (93)	226 (12)	630 (100)

of error and has been corrected for β -selenium by Marsh, Pauling & McCullough (1953) and for *p*-nitroaniline by Donohue & Trueblood (1956) (*cf.* comments by Abrahams & Robertson, 1956). The TC76 *y* coordinates for the atoms of the pyridinium ion are related to our values by $y_{TC76} = -1.14y_{BHK} - 0.09$ ($R^2 = 0.98$, where R is the regression coefficient) and those of the picrate ion by $y_{TC76} = -0.9y_{BHK} + 0.45$ ($R^2 = 0.70$). Thus, TC76 used a left-handed axial set and their ions were mutually shifted by ~ 0.5 along the short [010] axis. Using our $h0l$ intensities, we have satisfactorily refined the TC76 *x* and *z* coordinates to $R_{h0l} = 0.10$ (single overall temperature factor). We have not been able to refine the TC76 *y* and *z* coordinates. We have calculated distances between atoms in adjacent molecules using the TC76 coordinates; no short approaches were found and thus the error in their determination would be difficult to detect without comparison of observed and calculated F values of hkl reflections. The TC76 structure was included in the Cambridge Structural Database (RefCode PYRPIC) without comment. Further discussion in this paper refers only to our results.

2.3. Dependence of cell dimensions on temperature

A single crystal of phase I was sealed into a capillary and mounted on a Nonius crystal-heating device

(design of Tuinstra & Fraese Storm, 1978) modified for attachment to the Philips four-circle diffractometer. The temperature scale was calibrated by determining the melting points of a number of compounds at suitable intervals. Cell dimensions were measured using $MoK\alpha$ over the temperature range 293–353 K; the crystal showed signs of disintegration above 353 K. It is convenient to note here that similar measurements were made for phase II, up to a maximum of 393 K, above which temperature the single crystal disintegrated slowly to a powder. The values of a , b , c , β and V for both phases are given in Table E (deposited), and a diagram of V against T in Fig. 7 (see §7).

3. Determination of the crystal structure of phase II

3.1. Experimental

Crystals of phase I of pyridinium picrate (prepared as above) were heated, at a rate of $\sim 3 \text{ K min}^{-1}$, in a closed vessel to a few K above the melting point and then cooled to room temperature at the same rate. Yellow prisms were obtained; Debye-Scherrer photographs of powdered material confirmed that this was the high-temperature phase found in the phase-transformation studies (see below). If not held in a closed vessel, phase II was found to be stable at room temperature as single crystals for 2–3 weeks and thereafter disintegrated to a powder, but without change of phase (checked by Debye-Scherrer photography); presumably there had been some loss of pyridine.

As essentially the same experimental methods were used for the crystallographic studies of both phases, only differences will be mentioned. Crystal size was approximately $0.13 \times 0.24 \times 0.4 \text{ mm}$; 2280 reflection intensities were measured by the $\omega/2\theta$ scan method; the maximum value of $\sin \theta/\lambda = 0.595 \text{ \AA}^{-1}$ and the indices lay within the limits $-11 \leq h \leq 11$, $-10 \leq k \leq 10$, $0 \leq l \leq 8$. The crystal and measuring systems were stable to within 1.5% over the 60 h measuring period. The structure was refined using 1478 independent reflections with $F > 3\sigma(F)$, with weights equal to $2.31/(\sigma^2 F_{meas})$. The largest value of $|\Delta/\sigma|$ in the final refinement cycle was 0.10 (average value 0.005), and ρ_{max} and ρ_{min} in the final difference map were 0.31 and -0.31 e \AA^{-3} , respectively. The final value of R_F was 0.0716. Atomic parameters are in Table 2.

4. Molecular structure

The atomic numbering of the pyridinium and picrate ions is shown in Fig. 1, with dimensions as found in the two phases in Table 3. There are no significant differences between the more precise values for phase I and the less precise values for phase II; the slight bond-length shortening in phase II with respect to phase I is perhaps due to the absence of corrections for thermal librations (see the thermal-motion analysis below). Deviations from the

Table 2. Atomic parameters ($\times 10^4$) for phase II of pyridinium picrate [pyridinium C(1)P to H(NP); picrate C(1) to H(2)]

The values of U_{eq} (units of 10^{-4} \AA^2) were calculated following Fischer & Tillmanns (1988) and their e.s.d.'s following the isotropic and orthic approximation of Schomaker & Marsh (1983). The values of U_{iso} also have units of 10^{-4} \AA^2 .

	<i>x</i>	<i>y</i>	<i>z</i>	U_{eq}/U_{iso}
C(1)	5048 (5)	-457 (5)	2512 (7)	425 (13)
C(2)	3850 (4)	426 (5)	2951 (7)	414 (12)
C(3)	2695 (5)	-80 (5)	4076 (7)	410 (12)
C(4)	2633 (4)	-1518 (5)	4868 (7)	395 (11)
C(5)	3704 (5)	-2474 (5)	4516 (7)	427 (13)
C(6)	4851 (4)	-1954 (5)	3396 (7)	411 (13)
N(1)	3817 (5)	1936 (5)	2086 (7)	631 (14)
O(1)	4830 (4)	2598 (4)	1437 (6)	714 (13)
O(2)	2723 (5)	2451 (5)	1989 (9)	1372 (22)
N(2)	1411 (4)	-2040 (5)	6073 (6)	508 (11)
O(3)	507 (4)	-1153 (5)	6493 (6)	701 (11)
O(4)	1328 (4)	-3358 (4)	6629 (6)	714 (12)
N(3)	5957 (5)	-3009 (5)	3084 (7)	596 (14)
O(5)	5686 (4)	-4291 (4)	2840 (7)	866 (15)
O(6)	7054 (4)	-2603 (5)	3111 (10)	1320 (27)
O(7)	6105 (3)	-38 (4)	1479 (5)	555 (10)
H(1)	1947 (45)	501 (50)	4435 (64)	480 (140)
H(2)	3671 (42)	-3421 (50)	5037 (64)	450 (140)
NP	7584 (4)	2261 (5)	-241 (6)	476 (11)
C(1)P	8662 (5)	1418 (6)	-764 (8)	498 (14)
C(2)P	9816 (5)	2056 (6)	-1704 (9)	560 (16)
C(3)P	9850 (5)	3572 (6)	-2140 (9)	573 (16)
C(4)P	8737 (6)	4406 (6)	-1608 (9)	622 (18)
C(5)P	7592 (5)	3734 (6)	-649 (9)	566 (15)
H(1)P	8577 (43)	362 (51)	-349 (62)	500 (140)
H(2)P	10623 (64)	1453 (69)	-2052 (87)	1050 (230)
H(3)P	10709 (49)	4038 (53)	-2880 (68)	650 (160)
H(4)P	8767 (50)	5428 (60)	-1809 (74)	690 (170)
H(5)P	6772 (50)	4259 (54)	-187 (71)	660 (160)
H(NP)	6808 (54)	1696 (59)	288 (75)	720 (170)

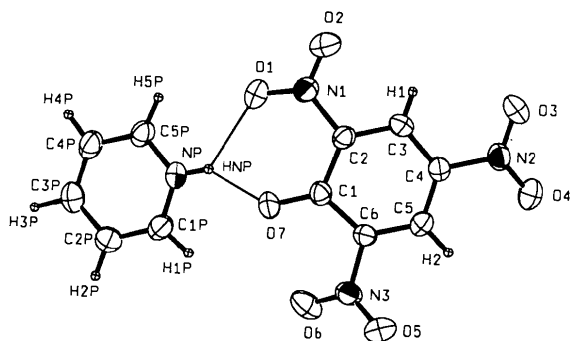


Fig. 1. ORTEP (Johnson, 1965) projection of pyridinium picrate ion pair viewed approximately down the normal to the mean plane of the pyridinium ion, showing numbering of the atoms. The thermal ellipsoids (given for phase I) are drawn at 50% probability values (this value is used for all ORTEP diagrams in this paper) and the mean C—H bond length is 0.96 (3) Å. The mean planes are defined throughout this paper (for each cell) with respect to the orthogonal right-handed axial set $X||a^*$, $Y||c^*$, $Z||c$, X , Y and Z in Å. For phase I, the equation of the mean plane of the pyridinium ion is $0.3707X - 0.9286Y + 0.0145Z - 1.3136 \text{ \AA} = 0$, and that of the benzene ring of the picrate ion is $0.2843X - 0.9112Y - 0.2980Z - 2.6777 \text{ \AA} = 0$. For phase II, the equation of the mean plane of the pyridinium ion is $0.3357X + 0.3065Y + 0.8907Z + 3.9091 \text{ \AA} = 0$, and that of the benzene ring of the picrate ion is $0.3037X - 0.1452Y + 0.9416Z - 3.7543 \text{ \AA} = 0$.

Table 3. Molecular dimensions ($\text{\AA}, ^\circ$) in the two phases of pyridinium picrate

Pyridinium ion	Phase I	Phase II
Bond lengths		
C(1P)—C(2P)	1.364 (4)	1.356 (7)
C(2P)—C(3P)	1.392 (4)	1.373 (7)
C(3P)—C(4P)	1.365 (4)	1.369 (7)
C(4P)—C(5P)	1.375 (4)	1.368 (7)
C(5P)—N(P)	1.330 (3)	1.336 (6)
C(1P)—N(P)	1.332 (3)	1.338 (6)
C(1P)—H(1P)	0.97 (3)	0.97 (5)
C(2P)—H(2P)	0.98 (3)	0.98 (6)
C(3P)—H(3P)	1.02 (3)	1.01 (5)
C(4P)—H(4P)	0.92 (3)	0.92 (5)
C(5P)—H(5P)	0.97 (3)	0.97 (5)
N(P)—H(NP)	0.84 (3)	0.92 (5)
Bond angles		
N(P)—C(1P)—C(2P)	120.2 (2)	120.5 (5)
C(1P)—C(2P)—C(3P)	118.7 (2)	118.6 (5)
C(2P)—C(3P)—C(4P)	119.4 (2)	120.2 (5)
C(3P)—C(4P)—C(5P)	120.0 (2)	119.6 (5)
C(4P)—C(5P)—N(P)	119.0 (2)	119.0 (5)
C(5P)—N(P)—C(1P)	122.7 (2)	122.1 (4)
Picrate ion		
Bond lengths		
C(1)—C(2)	1.447 (3)	1.450 (6)
C(2)—C(3)	1.379 (3)	1.367 (6)
C(3)—C(4)	1.379 (3)	1.376 (6)
C(4)—C(5)	1.388 (3)	1.382 (6)
C(5)—C(6)	1.368 (3)	1.364 (6)
C(6)—C(1)	1.451 (3)	1.449 (6)
C(2)—N(1)	1.450 (3)	1.459 (5)
C(4)—N(2)	1.448 (3)	1.449 (5)
C(6)—N(3)	1.462 (3)	1.456 (6)
C(1)—O(7)	1.248 (3)	1.241 (5)
N(1)—O(1)	1.228 (3)	1.195 (5)
N(1)—O(2)	1.224 (3)	1.212 (6)
N(2)—O(3)	1.223 (3)	1.225 (5)
N(2)—O(4)	1.224 (3)	1.223 (5)
N(3)—O(5)	1.227 (3)	1.215 (5)
N(3)—O(6)	1.223 (4)	1.192 (6)
C(3)—H(1)	0.85 (3)	0.92 (4)
C(5)—H(2)	0.94 (3)	0.91 (4)
O(1)—H(NP)	2.27 (3)	2.21 (5)
O(7)—H(NP)	1.93 (3)	1.86 (4)
Bond angles		
C(2)—C(1)—C(6)	111.8 (2)	111.0 (4)
C(1)—C(2)—C(3)	124.1 (2)	124.4 (4)
C(2)—C(3)—C(4)	119.2 (2)	119.3 (4)
C(3)—C(4)—C(5)	121.3 (2)	121.3 (4)
C(4)—C(5)—C(6)	118.9 (2)	118.7 (4)
C(5)—C(6)—C(1)	124.7 (2)	125.1 (4)
C(6)—C(1)—O(7)	123.0 (2)	122.9 (4)
C(2)—C(1)—O(7)	125.1 (2)	126.0 (4)
C(1)—C(2)—N(1)	119.7 (2)	119.3 (4)
C(3)—C(2)—N(1)	116.2 (2)	116.2 (2)
C(3)—C(4)—N(2)	119.5 (2)	119.0 (4)
C(5)—C(4)—N(2)	119.2 (2)	119.7 (4)
C(1)—C(6)—N(3)	118.6 (2)	118.6 (4)
C(5)—C(6)—N(3)	116.7 (2)	116.3 (4)
O(1)—N(1)—O(2)	121.9 (2)	122.1 (4)
O(3)—N(2)—O(4)	123.2 (2)	122.8 (4)
O(5)—N(3)—O(6)	123.5 (2)	123.0 (4)

Table 3 (*cont.*)

Torsion angles		
O(7)—C(1)—C(6)—N(3)	1.2	0.8
N(2)—C(4)—C(5)—H(2)	1.5	-1.4
O(7)—C(1)—C(2)—N(1)	-3.1	1.8
C(1)—C(2)—C(3)—C(4)	1.1	-0.3
C(2)—C(3)—C(4)—C(5)	-1.9	-1.4
C(3)—C(4)—C(5)—C(6)	1.4	2.0
C(4)—C(5)—C(6)—C(1)	0.0	-1.1
C(2)—C(1)—C(6)—C(5)	-0.7	-0.4
C(6)—C(1)—C(2)—C(3)	0.2	1.1
C(1)—C(6)—N(3)—O(6)	37.8	42.2
C(5)—C(6)—N(3)—O(5)	36.0	39.9
C(5)—C(4)—N(2)—O(4)	11.6	-5.6
C(3)—C(4)—N(2)—O(3)	12.1	-6.5
C(3)—C(2)—N(1)—O(2)	-20.1	-20.4
C(1)—C(2)—N(1)—O(1)	-20.2	-19.0
C(2)—N(1)—O(1)—H(NP)	4.8	25.8
N(1)—O(1)—H(NP)—O(7)	20.4	-14.4
O(1)—H(NP)—O(7)—C(1)	-44.9	-3.7
H(NP)—O(7)—C(1)—C(2)	46.8	8.6
O(7)—C(1)—C(2)—N(1)	-3.1	1.8

best plane of the six-membered ring of the pyridinium cation are given in Table B (deposited); this ring is non-planar in phase I, although only to a small extent ($\chi^2 = \Sigma(\Delta/\sigma)^2 = (180/13) = 13.8$, which is significant at better than the 0.5% level on 6-3 degrees of freedom). It can be described as very slightly boat shaped, with NP as one of the prow atoms. The less precise results for phase II do not show deviations from planarity.

Deviations from the best plane of the six-membered ring of the picrate anion of phase I are given in Table B (deposited); the ring is non-planar, although only to a small extent [$\chi^2 = \Sigma(\Delta/\sigma)^2 = (224/13) = 17.2$, which is significant at better than the 0.1% level on 6-3 degrees of freedom]. It can be described as very slightly boat shaped, with C(1) and C(4) as prow atoms. In phase II, the six-membered ring is not significantly non-planar ($\chi^2 = 4.4$). The phenolic O atom and the three N atoms are slightly but significantly displaced from the benzene ring plane in phase I. The nitro groups *ortho* to the phenolic O atom are rotated in opposite directions out of the benzene ring plane, with the hydrogen-bonded nitro group rotated about half as much as the other. The nitro O atoms adjacent to the phenolic O atom are displaced in the same direction with respect to the benzene ring plane. The disposition of the three atoms bonded to each of the N atoms is planar. Rather similar results were obtained for phase II, with small differences in detail. The most marked difference is in the opposite directions of rotation of the nitro group *para* to the phenolic O atom in the two phases (torsion angles in Table 3).

The ring bond lengths and angles show a pattern familiar from previous studies of picrate ions - the two C—C bonds adjacent to the phenolic O atom are longer, at ~ 1.45 Å, than standard C—C bonds in a benzene ring while the other four are very slightly shorter at ~ 1.38 Å. The major distortions of bond angles, from 120° , are in the region of the phenolic O atom, with smaller distortions around C(3). A discussion of the dimensions

of the picrate ion, based on information extracted from the Cambridge Structural Database and the more recent literature, is given below (§8).

The packing unit in the crystal in both phases is the hydrogen-bonded pyridinium-picrate ion pair, and we now describe the geometry of the interaction between these two moieties as found in phase I (Fig. 2), with values and comments for phase II given in square brackets. The ions of the pair are not coplanar, the angle between the planes of the pyridinium ring and that of the picrate benzene ring being 18.7° (9.9°). The hydrogen bond linking the cation and anion is bifurcated with a somewhat stronger linkage to the phenolic than to the nitro O atom [$d(\text{H} \cdots \text{O}) = 1.94$ compared with 2.27 Å (Table 3)] (corresponding values for phase II are 1.81 and 2.21 Å). The distances between the pyridinium N atom and the picrate O(7) and O(1) atoms are $2.632(3)$ and $2.929(3)$ Å [$2.662(6)$ and $2.871(6)$ Å], respectively. The six-membered chelate ring formed by the hydrogen bonding is non-planar (r.m.s. displacement = 0.19 Å); from the values of the torsion angles, this ring can be described (Boeyens, 1978) as having an approximate screw-boat form (r.m.s. displacement = 0.07 Å; the ring is also screw boat, but rotated with respect to that of phase I).

5. Crystal structure

A stereoview of the ion-pair arrangement in phase I is shown in Fig. 3; *parallel* ion pairs are superimposed

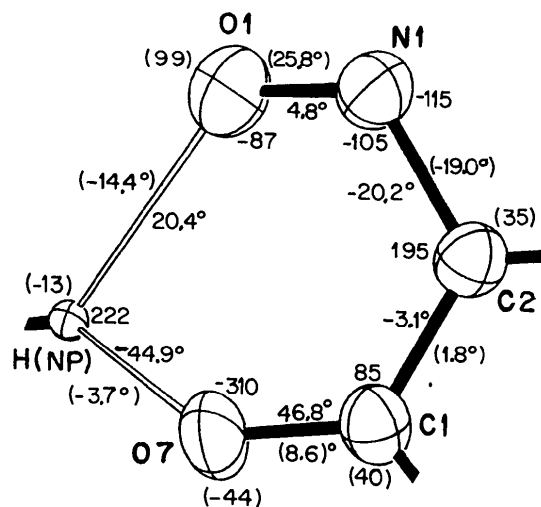


Fig. 2. View of the chelate ring between the hydrogen-bonded cation and anion of the ion-pair packing unit. The torsion angles ($^\circ$) and deviations from the mean plane (units of 10^{-3} Å) are shown. The values inside the ring refer to phase I and the circled values outside to phase II. The torsion angles are designated in a similar fashion. The equation of the mean plane of the chelate ring in phase I is $0.4536X - 0.8601Y - 0.2335Z - 0.3888 \text{ \AA} = 0$, while that in phase II is $0.3876X + 0.0167Y - 0.9217Z - 0.2844 \text{ \AA} = 0$, each with respect to the appropriate orthogonal axial system as described in the caption to Fig. 1.

along [110]; the stacks are arranged in the herringbone fashion typical of space group $P2_1/c$. There are only intramolecular hydrogen bonds and thus, in terms of arrangement of structural units, pyridinium picrate is a molecular crystal and not a salt. The intermolecular distances (Table C, deposited) are typical of van der Waals interactions. In phase II (Fig. 4) there are stacks of superimposed *antiparallel* ion pairs along [112]; pairs of stacks are related by the centres of inversion. Despite the large differences in cell dimensions for the two phases, the overall arrangements are similar in that both have quasi close packings of stacks of ellipsoidal cross-section; the differences stem from parallel ion pairs within a stack in phase I but antiparallel ion pairs in phase II and from the mutual arrangements of the stacks.

6. Thermal-motion analysis

The thermal motion in phase I has been partially analyzed with the program *THMA* (version of 15 April, 1987), using the rigid-body approximation [for a summary of recent developments in this area, see Dunitz, Maverick & Trueblood (1988) and Dunitz, Schomaker & Trueblood (1988)]. We could not obtain satisfactory

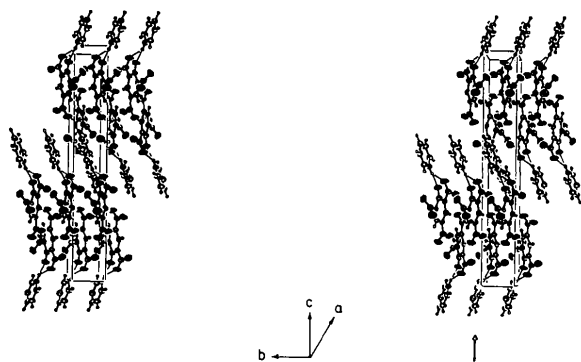


Fig. 3. ORTEP (Johnson, 1965) stereo diagram of the ion-pair arrangement in phase I viewed down [100], showing stacks of parallel ion pairs with [110] as the approximate stack axis. The standard ion pair (coordinates in Table 1) is indicated by an arrow.

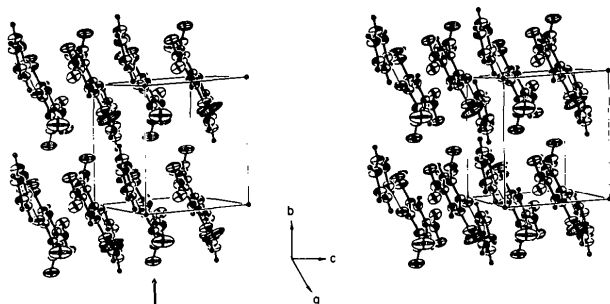


Fig. 4. ORTEP (Johnson, 1965) stereo diagram of the ion-pair arrangement in phase II viewed approximately down [100], showing stacks of parallel ion pairs with [112] as the approximate stack axis. The standard ion pair (coordinates in Table 2) is indicated by an arrow.

results for the pyridinium ion because of its symmetry (see acknowledgment below to Professor E. Maverick). The picrate ion was first analyzed as a rigid body and the R value obtained for observed and calculated values of U_{ij} for all non-H atoms was 0.155 \AA^2 . We then included libration of nitro groups about the C—N axes and R was reduced to 0.085; we report results only for this latter calculation. The eigenvector and eigenvalues are given in the inertial frame; the translational motion is almost isotropic (r.m.s. values: $T_1 = 0.179$, $T_2 = 0.172$, $T_3 = 0.161 \text{ \AA}$) and thus the directions of the translational principal axes with respect to the molecular axes are not well determined. Although the librational motions are rather anisotropic (r.m.s. values: $L_1 = 3.86$, $L_2 = 3.13$, $L_3 = 0.66^\circ$), there are no clear angular relationships to the molecular axes of inertia. The librational amplitudes of the three nitro groups are as follows: *ortho* (hydrogen bonded) 3.74° , *ortho* (not hydrogen bonded) 3.26° , *para* 2.22° , and the order is not as might be expected [*ortho* (hydrogen bonded) < *ortho* (not hydrogen bonded) < *para*]. Correction of bond lengths for librational motions adds $0.003\text{--}0.005 \text{ \AA}$ to C—C and C—N bond lengths and $\sim 0.02 \text{ \AA}$ to N—O bond lengths.

As for phase I, we could not obtain satisfactory results for the pyridinium ion in phase II because of its symmetry. The U_{equiv} values for phase II show large values for O(2) and O(6): reference to the Table of U_{ij} values (deposited) shows that these are due to values of 0.23 and 0.29 \AA^2 for U_{33} (in the crystal system) of atoms O(2) and O(6), respectively. The picrate ion was first analyzed as a rigid body and the R value obtained for observed and calculated values of U_{ij} for all non-H atoms was 0.227 . We then included libration of nitro groups about the C—N axes and R was reduced to 0.078 ; we report results only for this latter calculation. The large U_{33} values noted above are satisfactorily accounted for by the *THMA* analysis only when the libration of the nitro groups is included. The translational motion is rather isotropic (r.m.s. values: $T_1 = 0.207 \text{ \AA}$, $T_2 = 0.178 \text{ \AA}$, $T_3 = 0.167 \text{ \AA}$; see comment for phase I above). The librational motions are rather anisotropic (r.m.s. values: $L_1 = 5.49^\circ$ [almost about the C(1)—O(7) vector], $L_2 = 3.90^\circ$ [almost about an axis in the ring plane normal to C(1)—O(7)], $L_3 = 2.69^\circ$ (almost about the normal to the mean molecular plane); thus, the smallest libration is about the largest axis of inertia, as one might expect. The librational amplitudes of the three nitro groups are as follows: *ortho* (hydrogen bonded) 4.04° , *ortho* (not hydrogen bonded) 4.54° , *para* 5.42° , and the order is as might be expected. Correction of bond lengths for librational motions adds $0.005\text{--}0.008 \text{ \AA}$ to C—C and C—N bond lengths and $\sim 0.02\text{--}0.05 \text{ \AA}$ to N—O bond lengths.

It is well known that N—O bond lengths in nitro groups substituted in benzene rings show a fairly large range of values — for example, in the picrate ion and picric acid molecule of the complex carbamoyl-

choline picrate-picric acid (Jensen, 1975) the values of $d(\text{N—O})$, not corrected for thermal librations, range from 1.195(4) to 1.244(4) Å. Thus, correction for librational effects appears essential in order to obtain meaningful results. We give libration-corrected values for the picrate ion in phase I, averaged assuming that all C—N and N—O bond lengths are equal, and that the benzene ring has mirror symmetry: benzene ring: $d[\text{C}(1)—\text{C}(2)] = 1.453(6)$; $d[\text{C}(2)—\text{C}(3)] = 1.380(8)$; $d[\text{C}(3)—\text{C}(4)] = 1.386(6)$ Å; substituents: $d(\text{C—N}) = 1.458(6)$; $d(\text{N—O}) = 1.245(4)$; $d(\text{C—O}) = 1.251(-)$ Å.

We remark that $d(\text{N—O})$ in 1,2-dinitrobenzene takes up a mean value of 1.243 Å after correction for librational motion (Herbstein & Kapon, 1990).

7. Transition between the phases

Kofler's (1944) results have been summarized in the introduction; Kofler also noted that there was no weight loss even on long heating at 120° (presumably in a closed vessel). We have taken continuous Debye-Scherrer photographs of phase I as a function of temperature from 293–453 K; there is a transition at 383 K and the sample melts at ~443 K. If the sample is melted in a closed vessel and cooled slowly, then phase II crystallizes from the melt and can be cooled to 293 K without transforming to phase I; the occurrence of this process was confirmed by powder photography. Samples heated to ~453 K in an open system give confusing results. The enthalpies of transition and fusion were measured using a Mettler TA3000 DSC as $\Delta H_{\text{trans}} = 6.8$ and $\Delta H_{\text{fus}} = 31.2$ kJ mol⁻¹. Thus, the entropy of fusion is 70.5 J mol⁻¹ K. Kofler gives the temperature of the transition between the phases as 343 K, whereas we find

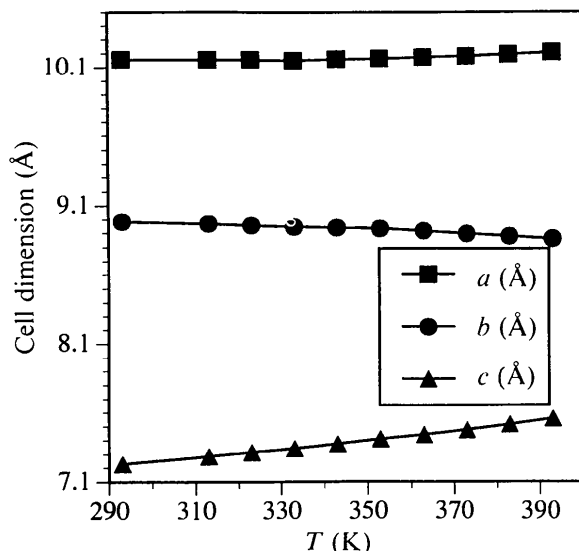


Fig. 5. Temperature dependence of cell edges for phase II. Stability ranges of the phases are discussed in the text.

383 K; we have noticed a distinct colour change at about 343 K when a sample is heated on a microscope hot stage. Presumably, it was the observation of this colour change that induced Kofler to assign too low a value to the transition temperature; its cause is not clear.

As noted above, cell dimensions have been measured as a function of temperature for both phases. The putative accessible range for phase I is 293–383 K but we have not been able to make satisfactory measurements

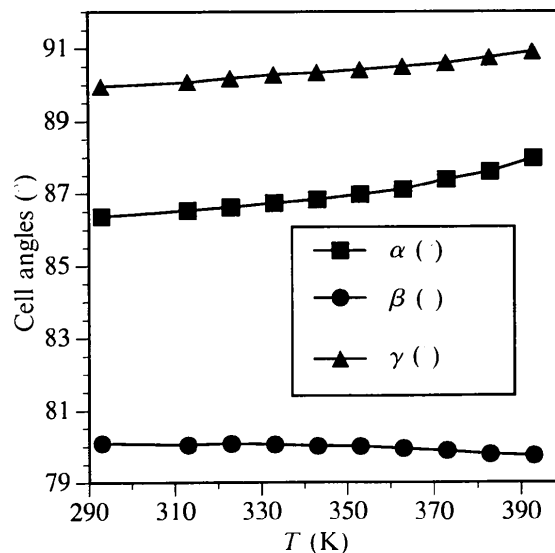


Fig. 6. Temperature dependence of cell angles for phase II. Stability ranges of the phases are discussed in the text.

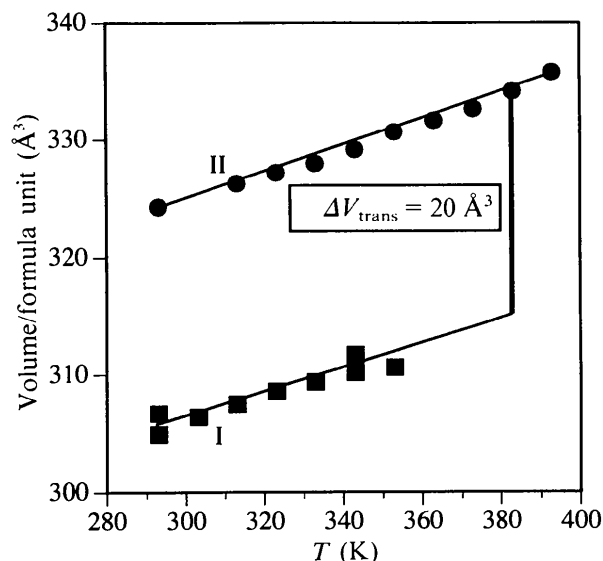


Fig. 7. Dependence of volume per formula unit on temperature for the two phases (phase II - upper curve, phase I - lower curve). Stability ranges of the phases are discussed in the text. The volume difference is constant (to a first approximation) over the temperature range shown.

Table 4. Symmetry-averaged bond lengths in the pyridinium ion

E.s.d.'s of individual values are $\approx 0.002\text{--}3 \text{ \AA}$.

Compound	$d(\text{C—N})$	$d[\text{C}(1)\text{—C}(2)]$	$d[\text{C}(2)\text{—C}(3)]$	Reference
Phase I	1.330	1.371	1.376	Present work
Phase II	1.339	1.362	1.370	Present work
Dipyridinium oxalate-oxalic acid	1.321	1.361	1.364	NTF85
Dipyridinium bis(hydrogen oxalate)-oxalic acid	1.329	1.355	1.377	NTF86
$\text{C}_5\text{H}_6\text{N}^+\cdot\text{F}^-\cdot\text{HF}$	1.338	1.378	1.389	BM88
$\text{C}_5\text{H}_6\text{N}^+\cdot\text{F}^-\cdot 2\text{HF}$	1.331	1.375	1.378	BM88
$\text{C}_5\text{H}_6\text{N}^+\cdot\text{Cl}^-$	1.332	1.364	1.384	MH89
$\text{C}_5\text{H}_6\text{N}^+\cdot\text{Cl}^-\cdot\text{HCl}$	1.345	1.375	1.388	MH89
$\text{C}_5\text{H}_6\text{N}^+$ (calc)	1.342	1.369	1.389	ATI89
$\text{C}_5\text{H}_5\text{N}\cdot\text{HF}$	1.339	1.368	1.371	BM88
$\text{C}_5\text{H}_5\text{N}$ (gas)	1.338	1.394	1.392	PHAGR87
$\text{C}_5\text{H}_5\text{N}$ (calc)	1.328	1.382	1.383	ATI89

References: NTF85, Newkome, Theriot & Fronczek (1985); NTF86, Newcome, Theriot & Fronczek (1986); BM88, Boenigk & Mootz (1988); MH89, Mootz & Hocken (1989); ATI89, Ajito, Takahashi & Ito (1989); PHAGR87, Pyckhout, Horemans, Alsenoy, Geise & Rankin (1987).

above $\sim 353 \text{ K}$ because of loss of diffraction. All the cell dimensions show a monotonic increase with temperature and the results have been deposited apart from the volume, which is shown in Fig. 7. We have been able to make measurements for phase II over the range 293–393 K. The a and c cell edges expand on heating while b contracts (Fig. 5); the behaviour of the angles is shown in Fig. 6. The cell volumes for both phases show monotonic increases with temperature (Fig. 7), the value of ΔV per formula unit remaining constant at $\sim 20 \text{ \AA}^3$ over the range 293–393 K.

In formal terms, the transformation of phase I into phase II requires rotation of alternate ion pairs in a stack by 180° about the normal plane so as to convert a parallel into an antiparallel stacking, and then additional, relatively minor, adjustments. Spatial considerations rule out a direct interconversion, so the transformation is expected to proceed by a nucleation and growth mechanism, and indeed diffraction photography shows that the transformation is from single crystal phase I to polycrystalline phase II. An open question is whether the ion pairs remain hydrogen bonded during this process, or break up and reform.

Burger & Ramberger (1979*a,b*) have proposed four rules governing the thermodynamic behaviour of polymorphs, two of which can be tested by our present results. These two rules are:

(1) Only an endothermic transition from a low- to a high-temperature polymorph is possible near a first-order transition point. A monotropic transition is exothermic. This is the heat of transition rule (HTR).

(2) The less stable polymorph will have the lower density at 0 K [the density rule (DR)].

Our results are compatible with both rules.

The transition between the phases is enantiotropic and first order (discontinuity in the volume-temperature curve) with an apparent transition temperature of 383 K, but is characterized by a large hysteresis in the sense that we have not (under our conditions) found phase II to transform to phase I on cooling. For example, a sample of phase II sealed into a capillary showed no change in its powder pattern when heated at 353 K for 24 h. The lack of reversibility suggests that there may be appreciable superheating above the true (thermodynamic) equilibrium temperature T_{eq} before the I to II transition occurs at a measurable rate. Such superheating has been found, for example, in *p*-dichlorobenzene (Mnyukh, 1976). Similarly, when II is cooled below T_{eq} the rate of the reverse reaction is very small. Values of T_{eq} have been determined, from the intersections of the solubility curves for the pairs of polymorphs, for thallium picrate by Rabe (1901) and for phthalylphenylhydrazide and phthalylphenylmethylhydrazide by Chattaway & Wunsch (1916). Our attempts to apply the same technique to pyridinium picrate have not been successful because of its relatively high solubility in the solvents available.

8. Mean dimensions of pyridinium and picrate ions

The value of ΔpK_a is 4.87 (pK_a for pyridine is 5.25 and 0.38 for picric acid) and the formation of a salt is in accordance with the conclusion of Johnson & Rumon (1965) that salts of the type $B^+H^+\cdot A^-$ are formed when $\Delta pK_a > 3.8$.

(a) The pyridinium ion: most previously measured values suffer from disorder or high thermal motion [see Newkome, Theriot & Fronczek, 1985, 1986 (NTF85, NTF86) for discussion of earlier work and references]. Our present values, averaged for C_{2v} -*mm2* symmetry, agree reasonably well with the values measured by Newkome *et al.* (Table 4) and more recent values from Boenigk & Mootz (1988; BM) and Mootz & Hocken (1989; MH). A structure has also been reported (Hensen, Pullmann & Bats, 1988) for a metastable phase of $\text{C}_5\text{H}_6\text{N}^+\cdot\text{Cl}^-$ but neither coordinates nor bond lengths were included in the paper. We note that some symmetry-related values differ significantly and conclude that there are probably systematic errors in at least some of the measurements. As noted above, we have not been able to correct our values for thermal libration effects.

Measured bond lengths for the pyridine molecule come from the crystallographic study of $\text{C}_5\text{H}_5\text{N}\cdot\text{HF}$, where it seems not unlikely that there is a systematic shortening of the values due to the absence of librational corrections, and, for the gas phase, from a combination of microwave spectroscopy (Mata, Quintana & Sorensen, 1977) and electron-diffraction measurements (Pyckhout, Horemans, van Alsenoy, Geise & Rankin, 1987; PHAGR87). The principal difference between molecule and cation seems to be that $d[\text{C}(1)\text{—C}(2)]$ is

Table 5. Average values of dimensions (\AA) of the picrate ion obtained from crystal structure determinations published in 1985 and thereafter

References are given in the text. Bond angles show equally good agreement with the Walkinshaw values and details are omitted.

Parameter	$d[\text{C}(1)-\text{C}(2)]$	$d[\text{C}(2)-\text{C}(3)]$	$d[\text{C}(3)-\text{C}(4)]$	$d(\text{C}-\text{O}^-)$	$d(\text{C}-\text{N})$	$d(\text{N}-\text{O})$
No. of independent values	18	18	18	9	27	54
Arithmetic mean	1.449	1.367	1.382	1.245	1.452	1.221
Sample s.d.	0.011	0.007	0.007	0.010	0.010	0.012
Range	0.041	0.025	0.024	0.034	0.047	0.071
Walkinshaw value	1.452 (9)	1.367 (10)	1.379 (10)	1.241 (11)	1.456 (12)	1.220 (8)

slightly shorter than $d[\text{C}(2)-\text{C}(3)]$ in the cation but these lengths are equal in the molecule; however, there remains a residual uncertainty of $\sim 0.01 \text{\AA}$ in the bond lengths of molecule and cation. Many *ab initio* self-consistent field molecular orbital calculations have been made for pyridine and the pyridinium ion and we give only the most recent results. Comparable results for ion and molecule were obtained using the program GAMESS with a 4-31G basis set (Ajito, Takahashi & Ito, 1989; ATI89); the small differences indicated by experiment are reproduced. A 3-21G-level calculation (GAUSSIAN82; Murray, Seminario & Politzer, 1989) gives essentially the same values for pyridine.

(b) The picrate ion: Walkinshaw (1986) has carried out a Cambridge Structural Database (CSD) search on 31 picrate ion structures (criteria for inclusion: no disorder, $R < 0.09$); average values, assuming that the benzene ring has mirror symmetry and that all C—N and all N—O bonds have equal lengths, are given in Table 5. These values are in excellent agreement (to within 0.01\AA , 1°) with those reported in the following more recent high-quality structure determinations. The picrates with interionic hydrogen bonding include choline picrate (Frydenvang & Jensen, 1992), mearsinium picrate (Robertson & Tooptakong, 1985), *N*(6)-methyladeninium picrate (Dahl & Riise, 1989), *N*(6),*N*(6)-dimethyladeninium picrate (Dahl, 1986), promethazine picrate (Venkataramana Shastry, Sheshadri, Shashidhara Prasad & Narayana Achar, 1987), kinetin picrate (Soriano-Garcia, Toscano & Espinosa, 1985; kinetin is 6-furfurylaminopurine), fenpropimorph picrate (Jensen & Jensen, 1990) and 3-hydroxy-4-methoxy-*N,N,N*-trimethylbenzene-ethanaminium (salicifoline) picrate (Wang, Cong & Liu, 1991), while ethyl 8-dimethylamino-1-naphthalene-carboxylate picrate (Parvez & Schuster, 1991) and muscarone picrate (Frydenvang, Jensen & Nielsen, 1992) are salts without interionic hydrogen bonding. Thus, the dimensions of the picrate ion are well established, with the caveat that $d(\text{N}-\text{O})$ should be 1.24\AA , after librational correction.

There is some variability in other geometrical features, presumably due to packing effects. The benzene ring is usually planar but there are a number of examples in which a slight boat shape is found, as in the present phase I. The N atoms of the nitro groups and the picrate

O atom are usually coplanar with the ring but deviations of up to 0.1\AA have been reported. The N atoms are always found to be coplanar with their three covalently linked atoms. The *para* nitro groups have torsion angles of up to 10° with respect to the ring plane but those of the *ortho* nitro groups depend on the details of the cation-anion hydrogen bonding, which can also involve the nitro O atoms, so it is difficult to generalize. The largest torsion angle we have encountered is 66° in promethazine picrate.

Dimensions are available for the picric acid molecule [neat picric acid (Duesler, Engelmann, Curtin & Paul, 1978; Srikrishnan, Soriano-Garcia & Parthasarathy, 1981); phenanthrene:picric acid (Yamaguchi, Goto, Takayanagi & Ogura, 1988); carbamoylcholine picrate:picric acid (Jensen, 1975)] so the geometrical changes that occur on ionization can be assessed. The only appreciable effects are those occurring in the vicinity of the C—O group. Although resonance structures can be invoked, it seems simplest to account for the changes on the basis of a redistribution of bonding electrons from the adjacent ring C—C bonds, which are lengthened (by 0.04\AA) on ionization, to the C—O bond, which is shortened by 0.02\AA . There is a concomitant reduction of about 4° in the C(6)—C(1)—C(2) angle on ionization.

9. Comparison with other picrate structures

The present structures have some resemblances to that of mearsinium picrate (Robertson & Tooptakong, 1985), which also has columns of discrete hydrogen-bonded ion pairs [$d(\text{N} \cdots \text{O}) = 2.686(2) \text{\AA}$]. The hydrogen bonding in mearsinium picrate is stronger than in pyridinium picrate [$d(\text{H} \cdots \text{O}) = 1.66(3)$ compared with $1.94(3)$ (phase I) and $1.81(4) \text{\AA}$ (phase II)]. Internally linked ion pairs are also found in the crystals of *N*(6),*N*(6)-dimethyladeninium picrate (Dahl, 1986), choline picrate (Frydenvang & Jensen, 1992), promethazine picrate (Venkataramana Shastry, Sheshadri, Shashidhara Prasad & Narayana Achar, 1987) and salicifoline picrate ($\text{OH} \cdots \text{O}$ hydrogen bond; Wang, Cong & Liu, 1991), while in *N*(6)-methyladeninium picrate (Dahl & Riise, 1989) and kinetin picrate (Soriano-Garcia, Toscano & Espinosa, 1985) such ion pairs are linked back-to-back with hydrogen bonds between the cations to give a

centrosymmetric four-moiety unit. It has been suggested that mixed stacking of alternating cations and anions in *N*(6),*N*(6)-dimethyladeninium picrate is evidence for charge-transfer interaction between them and this term has also been used in connection with promethazine picrate. As both of these crystals are yellow in colour, there does not seem to be supporting spectroscopic evidence.

10. Summary

The crystal structures of the two phases of pyridinium picrate (phase I, stable up to 373 K; phase II, stable from 373 K to the melting point of 441 K) have been determined from intensity measurements made at 298 K. The structure obtained for phase I corrects an earlier report. Thermal-motion analyses for the picrate ion in both phases show greater translation amplitudes in phase II (by factors of 1.16–1.03) and similarly for libration (by factors of 1.25–4.08); the libration amplitudes of the nitro groups about the C—N bonds are also greater in phase II (by factors of 1.08–2.44). The phase transition at 373 K is first-order enantiotropic but was not found to be reversible under our experimental conditions. The enthalpies of transition and fusion and the volume change on transition have been measured.

We are grateful to Professors H.-B. Bürgi (Bern) and Emily Maverick (UCLA) for advice regarding the use of *THMA*, Professor A. Siegmann (Materials Engineering, Technion) for access to the Mettler Differential Scanning Calorimeter, and the Vice President for Research and the Fund for the Promotion of Research at Technion for financial support. We acknowledge with thanks support for Dr Botoshansky from the Israel Ministry for Science and Technology, and that part of this work was carried out during tenure (by FHH) of a Foundation for Research Development Exchange Professorship in South Africa.

Note added in proof: Editorial checking has shown that the structure of phase I has been determined independently by Takayanagi *et al.* (1990). Their results and brief discussion agree well with ours, except for errors in their cell volume (given as 1124.5 instead of 1219.85 Å³) and calculated crystal density (given as 1.823 instead of 1.67 g cm⁻³), and in that different directions were chosen for the *y* axes ($y_{\text{BHK}} = 1 - y_{\text{TK}}$). We have checked that we used a right-handed coordinate system. The structure of 4b,5,15b,16-tetrahydrodibenzo[3,4:7,8][1,5]diazocino[2,1-*b*:6,5-*b'*]-diquinazoline-11,22-dium, [(TAABH₂)²⁺](picrate⁻)₂, has been determined (Owston & Shaw, 1988). The [(TAABH₂)²⁺] cation is hydrogen bonded to each of its two associated picrate ions forming units which interact with their neighbors only by van der Waals forces. The O···H—N distance (2.89 Å) is considerably longer than in pyridinium picrate; there is also a C—H···O interaction (3.12 Å).

References

- ABRAHAMS, S. C. & ROBERTSON, J. M. (1956). *Acta Cryst.* **9**, 966.
 AJITO, K., TAKAHASHI, M. & ITO, M. (1989). *Chem. Phys. Lett.* **158**, 193–198.
 BOENIGK, D. & MOOTZ, D. (1988). *J. Am. Chem. Soc.* **110**, 2135–2139.
 BOEYENS, J. C. A. (1978). *J. Cryst. Mol. Struct.* **8**, 317–320.
 BURGER, A. & RAMBERGER, R. (1979a). *Mikrochim. Acta*, pp. 259–271.
 BURGER, A. & RAMBERGER, R. (1979b). *Mikrochim. Acta*, pp. 273–316.
 CHATTAWAY, F. D. & WÜNSCH, D. F. S. (1916). *J. Chem. Soc.* **119**, 2253–2265.
 DAHL, T. (1986). *Acta Chem. Scand.* **B40**, 226–229.
 DAHL, T. & RIISE, B. (1989). *Acta Chem. Scand.* **43**, 493–495.
 DONOHUE, J. & TRUEBLOOD, K. N. (1956). *Acta Cryst.* **9**, 960–965.
 DUESLER, E. N., ENGELMANN, J. H., CURTIN, D. Y. & PAUL, I. C. (1978). *Cryst. Struct. Commun.* **7**, 449–453.
 DUNITZ, J. D., MAVERICK, E. F. & TRUEBLOOD, K. N. (1988). *Angew. Chem. Int. Ed. Engl.* **27**, 880–895.
 DUNITZ, J. D., SCHOMAKER, V. & TRUEBLOOD, K. N. (1988). *J. Phys. Chem.* **92**, 856–867.
 FISCHER, R. X. & TILLMANN, E. (1988). *Acta Cryst.* **C44**, 775–776.
 FRYDENVANG, K. & JENSEN, B. (1992). *Acta Cryst.* **C48**, 469–474.
 FRYDENVANG, K., JENSEN, B. & NIELSEN, K. (1992). *Acta Cryst.* **C48**, 1343–1345.
 HENSEN, K., PULLMANN, P. & BATS, J. W. (1988). *Z. Anorg. Allg. Chem.* **556**, 62–69.
 HERBSTSTEIN, F. H. & KAPON, M. (1990). *Acta Cryst.* **B46**, 567–572.
 JENSEN, B. (1975). *Acta Chem. Scand.* **B**, **29**, 891–903.
 JENSEN, J. S. & JENSEN, B. (1990). *Acta Cryst.* **C46**, 779–781.
 JOHNSON, C. K. (1965). *ORTEP*. Report ORNL-3794, Oak Ridge National Laboratory, Tennessee, USA.
 JOHNSON, S. L. & RUMON, K. A. (1965). *J. Phys. Chem.* **69**, 74–86.
 KOFLER, A. (1944). *Z. Elektrochem.* **50**, 200–207.
 MARSH, R. E., PAULING, L. & McCULLOUGH, J. D. (1953). *Acta Cryst.* **6**, 71–75.
 MATA, F., QUINTANA, M. J. & SORENSEN, G. O. (1977). *J. Mol. Struct.* **42**, 1–5.
 MNYUKH, YU. V. (1976). *J. Cryst. Growth*, **32**, 371–377.
 MOOTZ, D. & HOCKEN, J. (1989). *Z. Naturforsch. Teil B*, **44**, 1239–1246.
 MURRAY, J. S., SEMINARIO, J. M. & POLITZER, P. (1989). *J. Mol. Struct.* **187**, 95–108.
 NEWKOME, G. R., THERIOT, K. J. & FRONCZEK, F. R. (1985). *Acta Cryst.* **C41**, 1642–1644.
 NEWKOME, G. R., THERIOT, K. J. & FRONCZEK, F. R. (1986). *Acta Cryst.* **C42**, 1539–1541.
 OWSTON, P. G. & SHAW, L. S. (1988). *Acta Cryst.* **B44**, 39–50.
 PARVEZ, M. & SCHUSTER, I. I. (1991). *Acta Cryst.* **C47**, 446–448.
 PYCKHOUT, W., HOREMANS, N., ALSENOY, C. VAN, GEISE, H. J. & RANKIN, D. W. H. (1987). *J. Mol. Struct.* **156**, 315–329.
 RABE, W. O. (1901). *Z. Phys. Chem.* **38**, 175–184.
 ROBERTSON, G. B. & TOOPTAKONG, U. (1985). *Acta Cryst.* **C41**, 1332–1335.
 SCHOMAKER, V. & MARSH, R. E. (1983). *Acta Cryst.* **A39**, 819–820.
 SHELDRIK, G. M. (1976). *SHELX76. A Program for Crystal Structure Determination*. Univ. of Cambridge, England.
 SHELDRIK, G. M. (1986). *SHELXS86. A Program for Crystal Structure Solution*. Univ. of Göttingen, Germany.
 SORIANO-GARCIA, M., TOSCANO, R. A. & ESPINOSA, G. (1985). *J. Cryst. Spectr. Res.* **15**, 651–662.
 SRIKRISHNAN, T., SORIANO-GARCIA, M. & PARTHASARATHY, R. (1981). *Z. Kristallogr.* **151**, 317–323.
 TAKAYANAGI, H., KAWAOKA, R., CHIN, K., GOTO, M., YAMAGUCHI, S. & OGURA, H. (1990). *Anal. Sci.* **6**, 321–322; *Chem. Abstr.* **113**, 68713s.
 TALUKDAR, A. N. & CHAUDHURI, B. (1976). *Acta Cryst.* **B32**, 803–808.
 TUINSTR, F. & FRAASE STORM, G. M. (1978). *J. Appl. Cryst.* **11**, 257–259.
 VENKATARAMANA SHASTRY, C. I., SHESHADRI, T. P., SHASHIDHARA PRASAD, J. & NARAYANA ACHAR, B. (1987). *Z. Kristallogr.* **178**, 283–288.
 WALKINSHAW, M. D. (1986). *Acta Cryst.* **C42**, 246–249.
 WANG, Y., CONG, Q. & LIU, Y. (1991). *J. Cryst. Spectr. Res.* **21**, 385–389.
 YAMAGUCHI, S., GOTO, M., TAKAYANAGI, H. & OGURA, H. (1988). *Bull. Chem. Soc. Jpn.* **61**, 1026–1028.